'Photogrammetric Week '95', D. Fritsch & D. Hobbie, Eds., Wichmann Verlag, Heidelberg, 1995

Extraction of Semantic Information from MOMS-02/D2 Image Data

HERMANN KAUFMANN and MICHAEL BERGER, Potsdam

ABSTRACT

The Modular Optoelectronic Multispectral/Stereo Scanner (MOMS-02) is a newly designed sensor that provides multispectral coverage in 4 wavebands including the visible and near-infrared range. It is also equipped with a three line along-track stereo device, recording for/aft and high resolution nadir panchromatic data. Data acquired during the STS-55/D2 have been investigated with regard to their technical performance and spectral significance to validate the design of bands derived from theoretical considerations and modelling. To meet the objective, raw data have been preprocessed and coefficients for absolute calibration are provided. With some limitations, calculated results for radiometry, entropy, SNR and LSF performances are comparable to operational sensors. Results of variance/covariance analyses indicate a 10-15% improved spectral decorrelation for MOMS-02 bands as compared to those of operational sensors with broader band design.

1. INTRODUCTION

MOMS-02, was developed by MBB, now Daimler Benz Aerospace (DASA), (Meißner et. al., 1993) under contract to the German Space Agency (DARA) and the German Aerospace Research Establishment (DLR). MOMS-02 has been designed under consultancy of a scientific user group of different universities and research centers (Ackermann et. al., 1989). The new arrangement of centers and widths of spectral and panchromatic bands is discussed in Kaufmann et.al. (1989). MOMS-02 is financed by the German Federal Ministry for Education, Research and Technology (BMBF).
The instrument was first flown during the D2 mission aboard Space Shuttle flight STS-55. During a 9 days period in April/May 1993, approximately 8 mio. km^2 of data have been recorded in different modes from a mean altitude of 296km that results in a GIFOV of 4.5m x 4.5m for the nadir looking panchromatic HR module and 13.5m x 13.5m for the multispectral - and tilted panchromatic modules (Bodechtel et al., 1994). In the beginning of 1996, the system will collect data for 18 months on the Russian MIR station during the PRIRODA mission.
Main advanced performance capabilities of the MOMS-02 system are as follows:

- along-track three-fold stereo acquisition,
- high resolution panchromatic capability,
- narrow banded multispectral VIS/NIR design.

2. DESIGN OF MOMS-02 BANDS

2.1 Spectral Bands

The selection of spectral bands is limited due to the complexity of parameters such as ground pixel size, detector quantum efficiency, optics transmission, atmospheric effects, signal to noise ratio, data storage, etc. Within this given and hardware restrictions and based on spectra of natural surfaces, we were able to accommodate four relatively narrow bands in the visible and NIR range (Kaufmann et.al., 1989). This section of the electromagnetic spectrum is characterized by the high reflectance of vegetation (mesophyll) in the NIR and the steep falloff towards the visible due to strong pigment absorptions such as chlorophyll in the red region and chlorophyll/carotenoid in the blue range.
The spectral reflectance of minerals in this region is mainly influenced by the wings of charge transfer bands centered in the ultraviolet and crystal field absorptions at longer wavelengths, which are caused by transition elements. The most important transition element for terrestrial remote sensing purposes is iron in the bi- and trivalent state.

'Photogrammetric Week '95', D. Fritsch & D. Hobbie, Eds., Wichmann Verlag, Heidelberg, 1995

For selecting the center and width of spectral bands, in-vivo measurements of needles and leaves for different species of coniferous and deciduous trees in healthy condition and progressive states of senescence or stress have been carried out. In addition, minerals, rocks and soils of several arid test sites containing $Fe^{2+/3+}$ ions have been measured and analyzed.
To evaluate the energy available at specific wavelengths and to correct for the different attenuations due to atmospheric water vapor and molecular oxygen, the solar spectral irradiance (Wolfe and Zissis, 1978) and an atmospheric model, LOWTRAN code (Kneizys et al., 1988), were utilized to calculate the incoming radiation based on standard parameters for path, latitude, season, visibility, etc. Proper gain settings and aperture has been calculated by Richter and Lehmann (1989).
Finally, band centering and width has been modelled with regard to the spectral characteristics of vegetation, minerals, rocks and soils, respectively, especially their causal factors as pigments and $Fe^{2+/3+}$ (Kaufmann et al. 1989). The resulting spectral bands have been as follows: Band 1: 449nm-511nm; Band 2: 532nm-576nm; Band 3: 645nm-677nm; Band 4: 772nm-815nm. Nominal and effective band-passes are displayed in figure 1.

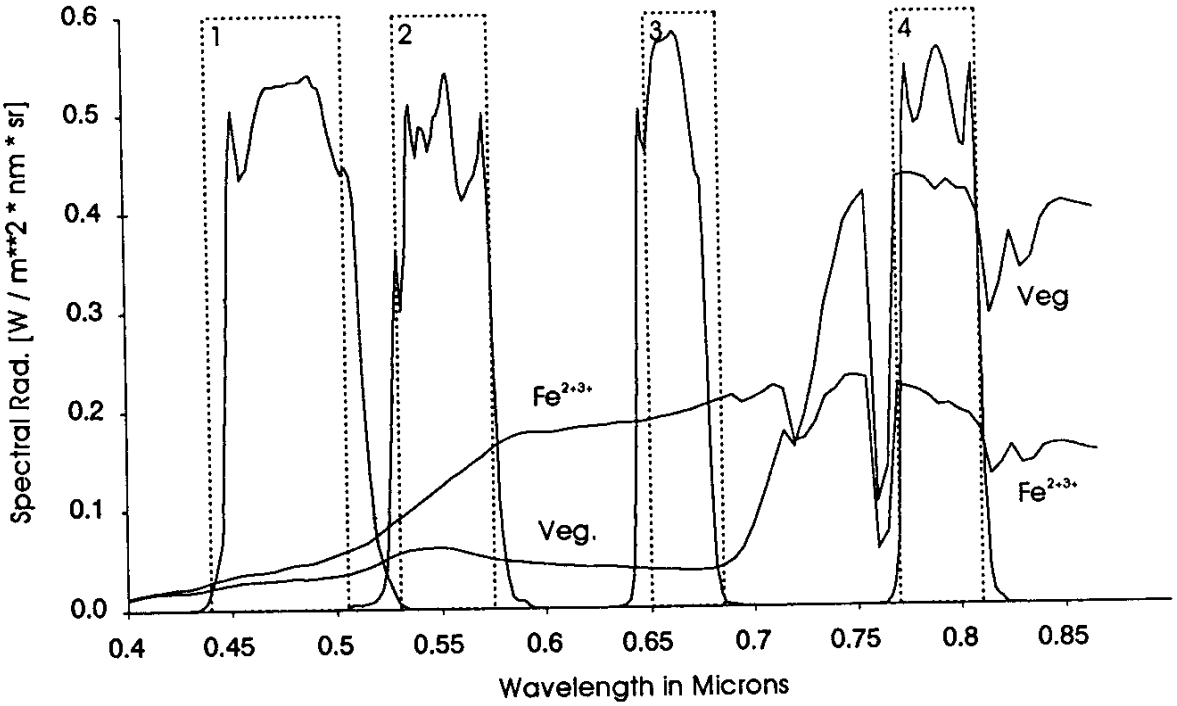

Figure 1: Nominal (dotted blocks, related to 100% transmission) and effective band-passes of MOMS-02 multispectral bands. Also shown are mean radiance spectra of chlorophyll (Veg) and $Fe^{2+,\ 3+}$-bearing (Fe) targets used for the design of bands.

2.2 Panchromatic Bands

Panchromatic bands are used for three-line stereo data acquisition (high resolution nadir (band 5) and for/aft (bands 6, 7) modules). To design the filter for a panchromatic band, one has to take into account the contrast in apparent albedo of vegetation and rock/soils within a range, covering the VIS and NIR wavebands. These are dominated by the steep increase of reflectance of vegetation canopies at the red edge at around 700nm. Therefore, is was decided to optimize the band-passes in extending the right edge into the longer wavelength. This was to avoid most of the noise and low-pass characteristics introduced by atmospheric scattering at shorter wavelengths and to display vegetation in sufficient brightness in internal contrast and to bare soils. The resulting filter was 512nm-765nm (nominal: 520nm-760nm) with slight variations for the tilted modules.

'Photogrammetric Week '95', D. Fritsch & D. Hobbie, Eds., Wichmann Verlag, Heidelberg, 1995

3. VALIDATION OF DESIGNED BANDSURE

The validation of MOMS-02 data is based on imagery taken during the STS-55/D2 mission. To derive a measure of the instruments in-flight performance, several algorithms and approaches have been used. Data investigated are compared with operational sensors. Mainly due to thermal problems and periodical malfunctions of parts of the electronic equipment, quality of this experimental data can vary significantly from one orbit to another. For performance analysis data of two different orbits were selected that have been recorded to the start and at the end of the mission.
One area is located in Saudi Arabia (arid climate), the second one in Zimbabwe (sub-tropical climate). Due to the high transmission rate, data have been recorded in different modes. MOMS-02 data of Saudi Arabia (Orbit No: 28) were recorded in mode II (all multispectral bands), data of Zimbabwe (Orbit No: 126) were recorded in mode VI (3 multispectral bands and the highly resolving, panchromatic nadir band). The following table (1) lists the data investigated:

SENSOR	ORBIT / PATH-ROW	DATE OF ACQ.
MOMS-02/D2	126 Scene 5 & 6	May, 4th. 1993
MOMS-02/D2	28 Scene 10 & 11	April, 28th. 1993
TM/LANDSAT-5	170/ 72	April, 12th. 1993
TM/LANDSAT-5	172/ 41	July, 6th. 1984
SPOT-HRV	134/386	May, 14th. 1993

Table 1: Investigated sets of data.

4. FOURIER ANALYSIS

MOMS-02 raw data have been analysed using a Fast Fourier Transformation (FFT). Besides an odd/even effect in flight direction (different read-out electronics) a three-line effect in scan direction (multiplexer problem) occurs. Most of these stripping can be seen in band 3. It is responsible for the noisy visual impression. In all bands (especially in the panchromatic data) saturated white pixels as well as unsaturated black pixels are repeatedly present. Furthermore an non periodical scan-line shift of 4 pixels occurs.
Most of these effects are due to unstable temperature condition during the shuttle mission and vary between data-takes and from scene to scene. Due to the low orbit altitude of the shuttle the read-out frequency of the shift registers were driven over their specifications (5Mhz instead of 4Mhz). Thus, linear operation could not be provided and small changes in temperature caused different voltage outputs for equal radiance inputs. This problem will vanish driving the sensor at lower read-out frequency e.g. at higher orbit altitudes as it will be the case for e.g. the PRIRODA mission. Furthermore, electronic parts have been changed and additional shielding will provide stable temperature conditions in future missions.

5. DATA PRE-PROCESSING AND RECTIFICATIONTION

An adapted histogram matching algorithm was applied to MOMS-02 raw data which gave reasonable results correcting the odd/even effect and multiplexer problem. Each image was divided into 6 subscenes to separate the striping effects. Radiometric calibration was applied by matching the subscenes to the scene with the highest mean level. Thereafter the subscenes were remerged.
Besides this a Fourier filtering using sharp ideal filters was tested. Due to the loss of information as well as the occurrence of interferences the histogram matching method was preferred.
The multispectral bands are not registered perfectly to each other, which is due to a minimum bend of the center plate where the multispectral lenses are mounted. Band 1 and band 2 are shifted 7 pixels in

scan and 5 pixels in flight direction against band 3 and band 4. The accuracy of the band to band registration can slightly vary from scene to scene indicating an instability of the focal plane (center plate) during the mission. The shift can also be due to 'blind' elements of the CCD arrays.
Since analysis is based on recorded mission data, a comparison to complementary data of operational sensors like HRV and TM, recorded at similar acquisition dates, seems to be a reasonable approach. However, one has to keep in mind that radiometric and geometric preprocessing as well as resampling of multisensor data is critical and results present a relative measure of performance.
To meet the objective, LANDSAT-TM and SPOT-HRV images have been co-registered to MOMS-02 data sets and been resampled to equal ground pixel sizes using a polynomial of first degree and the nearest neighbour resampling method, to preserve the radiometry of the original data. The root mean square error was less than one pixel. Sun elevation correction was done using the cosine law under the assumption of the Earth being a Lambertian reflector. Furthermore a broad atmospheric correction was applied by cutting the histograms at the 3σ level.

6. ABSOLUTE CALIBRATION

To estimate the dynamic range of MOMS-02 and coefficients (C_0, C_1) for a transfer function to convert gray values (digital numbers (DNs)) to spectral radiance (L_λ), suitable subscenes of complementary TM data have been used. Assuming, the atmospheric conditions did not change significantly during the three weeks time difference in data recording, the TM data have been normalized to MOMS-02 data and converted to radiance values using the following formula:

$$L_\lambda = (((Lmax_{\lambda,i} - Lmin_{\lambda,i}) / 255) * DN_i + Lmin_{\lambda,i}) * Norm_i \quad (1)$$

where

L_λ	=	Spectral radiance
$Lmin_{\lambda,i}$	=	Spectral radiance at DN 0 for band 'i'
$Lmax_{\lambda,i}$	=	Spectral radiance at DN 255 for band 'i'
$Norm_i$	=	Normalization factor for band 'i'

The normalization factor $Norm_i$ for band 'i' is given by:

$$Norm_i = \frac{\int_{\lambda_{min,i}}^{\lambda_{max,i}} (L_{MOMS}(\lambda, \rho_i) \cdot R_{MOMS}(\lambda)) d\lambda \int_{\lambda_{min,i}}^{\lambda_{max,i}} R_{TM}(\lambda) d\lambda}{\int_{\lambda_{min,i}}^{\lambda_{max,i}} (L_{TM}(\lambda, \rho_i) \cdot R_{TM}(\lambda)) d\lambda \int_{\lambda_{min,i}}^{\lambda_{max,i}} R_{MOMS}(\lambda) d\lambda} \quad (2)$$

where

$R(\lambda)$	=	Response function of respective optics
$L(\lambda,\rho_i)$	=	Spectral radiance by a given sun-sensor geometry (sun elevation, orbit/target altitude), a standard atmosphere and an albedo 'ρ' different for each band 'i' (used values for ρ: ρ_{band2}=0.08, ρ_{band3}=0.03, ρ_{band4}=0.2).

Radiance values needed, have been calculated by the LOWTRAN atmospheric model using input parameters for the specific test-site, target/orbit height and response functions of optics as well as different albedo values for each band (Kneizys et al., 1988). Average albedo of vegetation has been used for normalization purposes. $Lmin_\lambda$ and $Lmax_\lambda$ for TM data are taken from Richter (1994). Parameters for the specific HRV scene (variable gain settings) could not yet be provided by SAC/RSA receiving station.

DNs of 'spectrally neutral' areas with different albedos (water, sands, concrete etc.) have been selected in MOMS-02 data and plotted versus normalized TM radiance values. To estimate the coefficients of the MOMS-02 transfer function, a linear regression analysis was applied. Furthermore, coefficients have been normalized by the gain settings (gain = $(2^{1/2})^{\text{gain setting}}$) of the specific data take. Results are listed in table 2. Assuming linearity within the entire dynamic range, absolute radiance values can be calculated from MOMS-02 digital numbers using the following formula.

$$L_\lambda = c_{0,i} + \frac{c_{1,i}}{\sqrt{2}^{GainSetting_i}} \times DN_i \qquad (3)$$

These results are valid for the investigated scene in first approximation. The presented coefficients may also be used to calculate radiance values of other MOMS-02 scenes (Berger and Kaufmann, 1995). However, due to problems with dark current subtraction and unstable thermal conditions of the MOMS-02 environment during the STS-55 mission, the significance of those results is somewhat reduced.

MOMS Band	C_0 [$Wcm^{-2}ster^{-1}\mu m^{-1}$]	C_1 [$Wcm^{-2}ster^{-1}\mu m^{-1}$]
2	$0.48 * 10^{-3}$	$0.42 * 10^{-3}$
3	$-1.00 * 10^{-3}$	$0.98 * 10^{-3}$
4	$-1.70 * 10^{-3}$	$0.37 * 10^{-3}$

Table 2: Coefficients of MOMS-02 transfer function.

7. SEMANTIC DATA EVALUATION

7.1 Signal to Noise Ratios

An automated estimate of the signal to noise ratios (SNR) similar as described in Bo-Cai (Bo-Cai, 1993) was used. For this purpose the images were subdivided in blocks of different pixel sizes (3x3, 4x4, 5x5,...). For each block the local standard deviation was calculated. Homogeneous blocks have small standard deviations while inhomogeneous blocks, such as those containing edges and texture features, have large standard deviations. Furthermore, the histogram of the local standard deviations were Gaussian fitted. Thus, the mean noise of the image is defined at the center of the Gaussian fit. SNR's were calculated by rationing the mean of the entire image by the mean noise. The SNR's for each band were plotted versus the block sizes and used to estimate the SNR's. Due to the applied nearest neighbour resampling method only block sizes multiplied by the resampling factor have been used. Table 3 lists the results of relative SNRs of the Zimbabwean orbit (scene1 - 698x1253 pixels, scene 2 - 1647x1185 pixels, both mode VI) and of 2 subscenes of the Saudi Arabian orbit (scene 3, 6293x4161 pixels, scene 4, 6820x4529 pixels, both mode II).
The Zimbabwean data were recorded after the rainy period and during the harvesting season. The season implies a change of the vegetation cover within a few days. TM and HRV data have not been available for the same day of the STS-55 overflight and therefore the results are not directly comparable. The SNR's of the MOMS data in the NIR seem to be much higher which might be due to more homogeneous vegetation covered areas which on the other hand absorb in band 2 and 3 and results in a much lower SNR in these bands. Furthermore, the amount of small patterns had to be taken into consideration. The smaller the patterns and the higher the spatial resolution the lower are the calculated SNR's. Numerous small patterns are present in scene 1 and 2 e.g. small scale farming areas, the City of Harare with its suburbs and the township of Chitungwiza.
A comparison is provided with the results of the arid scenes (scene 3 and 4). MOMS SNR's are slightly less than the SNR's of the TM sensor besides MOMS band 3. This is due to gain setting (commanding)

'Photogrammetric Week '95', D. Fritsch & D. Hobbie, Eds., Wichmann Verlag, Heidelberg, 1995

problems during the mission. Taken into account the former mentioned thermal conditions and electronic malfunctions, and the basic corrections applied, the results can be classified very satisfying.

	Scene 1	Scene 2	Scene 3	Scene 4	Mean
MOMS/HRV					
2/1	0.57	0.87	-	-	N/A
3/2	0.56	0.73	-	-	N/A
4/3	1.61	1.80	-	-	N/A
MOMS/TM					
1/1	-	-	0.92	1.15	1.04
2/2	0.55	0.81	0.90	0.84	0.87
3/3	0.59	0.69	0.56	0.48	0.52
4/4	1.36	1.44	0.98	1.03	1.01

Table 3: Relative SNRs.

7.2 Entropy

The entropy, a quantitative measure of image information content, was calculated using the following formula:

$$H = -\sum_{i=0}^{255} p(i) \log_2 p(i) \qquad (4)$$

where p(i) is the probability of the occurrence of the digital number (DN) with the value i. Thus p(i) is defined as the frequency of DN i divided by the total of all pixels in the image.The relative entropy was calculated by rationing the entropy of corresponding bands.

	Scene 1	Scene 2	Scene 3	Scene 4	Mean
MOMS/HRV					
2/1	1.13	1.08	-	-	1.11
3/2	0.89	0.91	-	-	0.90
4/3	0.96	0.97	-	-	0.97
MOMS/TM					
1/1	-	-	0.91	0.93	0.92
2/2	1.27	1.16	0.99	0.99	1.10
3/3	0.96	0.91	0.79	0.76	0.86
4/4	0.97	0.97	0.91	0.91	0.94

Table 4: Relative Entropy.

Table 4 lists the relative entropy of 2 subscenes (see explanations for table 2). The results of the MOMS-02 bands are comparable to operational sensors and differ at a maximum of 0.5 bits/pixel. MOMS band 3 of the arid scenes (scene 3 and scene 4 - Saudi Arabia) differs about 1.5 bits/pixels versus TM3 (see SNR).

'Photogrammetric Week '95', D. Fritsch & D. Hobbie, Eds., Wichmann Verlag, Heidelberg, 1995

7.3 Line Spread Function

The line spread function (LSF) was estimated by extracting profiles over three well known sharp edges. Five profiles in different directions were extracted. The first deviation of each profile was Gaussian fitted under the assumption that the LSF will have a Gaussian distribution (Hallada et. al., 1986). Thus the LSF is defined by the half width of the Gaussian fit. Per edge the mean of LSF`s were calculated. Table 5 lists the results in pixel units with the corresponding standard deviations.

	MOMS				HRV			TM			
Band	1	2	3	4	1	2	3	1	2	3	4
Mean LSF [Pixel]	1.62	1.73	1.44	1.76	1.16	1.96	1.51	1.25	1.33	1.57	1.45
St.Dev.	0.31	0.22	0.17	0.33	0.21	0.32	0.20	0.23	0.33	0.18	0.23

Table 5: LSF-values.

Considering the standard deviations, the LSF's are within comparable ranges. The slightly blurred visual impression of MOMS band 4 does not show up in calculation. The LSF of MOMS-02 is rather satisfying as compared to data of the predecessor MOMS-01.

7.4 Correlation of Spectral Bands

To investigate the significance of spectral variations of MOMS versus HRV/TM, several sections of the arid area of Saudi-Arabia (TM) and vegetated sites of the Zimbabwe orbit have been selected. Besides visual inspection that shows more saturated colors for MOMS-02 composites, two quantitative methods have been applied: interband correlation techniques and IHS-transformation. Cross-correlation, variances of eigenvalues, and calculated saturation components clearly indicate an improvement of spectral decorrelation for MOMS-02 bands by 10-15% for $Fe^{2+, 3+}$ targets. %). This is in accordance with simulation results based on high resolving lab-spectra of rock samples (Kaufmann et al., 1989).
Bands of vegetated targets show improvements of up to 25%, as predicted by Koch et. al. (1993). Due to harvesting activities and thus change in phenology during the time gap of acquisition (Tab. 1) these results can just be seen as estimates and need further investigation. However, the results are very satisfying and confirm the advantages of the new arrangement of the band centers and widths.

7.5 Visual Inspection of Panchromatic Band

Figures 2a,b and 3a,b show co-registered panchromatic bands of the HRV and MOMS-02. Both sets are sections of the Zimbabwe orbit 126, displaying a high density suburb south of the capital Harare (Fig.2) and a farming area with different vegetation and dams, reservoires and greenhouses (Fig.3). Besides the different spatial resolution of data, the internal contrast reflects the different 'philosophies' of design. The HRV band shows a strong contrast of soils to vegetation, but the later is hardly to be differentiated and can be confused with water surfaces and wet areas. The MOMS-02 band displays vegetation bright and accentuated, but with less contrast to soils.

'Photogrammetric Week '95', D. Fritsch & D. Hobbie, Eds., Wichmann Verlag, Heidelberg, 1995

Figure 2a: HRV panchromatic band of high density suburb south of Harare. GIFOV:10m x 10m. Range: 510nm-730nm. Linear stretch, histogram cut-off at ± 2.5σ.

Figure 2b: MOMS-02 panchromatic band. GIFOV: 4.5m x 4.5m. Range: 512nm-765nm. Linear stretch, histogram cut-off at ± 2.5σ. Note the increasing apparent albedo and transparence of vegetated areas.

Figure 3a: HRV panchromatic band of farming area south of Harare. GIFOV:10m x 10m. Range: 510nm-730nm. Linear stretch, histogram cut-off at ± 2.5σ.

Figure 3b: MOMS-02 panchromatic band. GIFOV: 4.5m x 4.5m. Range: 512nm-765nm. Linear stretch, histogram cut-off at ± 2.5σ. Note the increasing apparent albedo and transparence of vegetated areas.

'Photogrammetric Week '95', D. Fritsch & D. Hobbie, Eds., Wichmann Verlag, Heidelberg, 1995

8. ACKNOWLEDGMENTS

The MOMS scientific program is funded by the German Federal Ministry for Education, Research and Technology (BMBF).

9. REFERENCES

Ackermann, F., J. Bodechtel, E. Dorrer, H. Ebner, H. Kaufmann, B. Koch, G. Konecny, F. Lanzl, P. Seige, H. Winkenbach, and J. Zilger, (1989): MOMS-02 D2 Wissenschaftsplan. DLR, Oberpfaffenhofen, FRG, 81 pp.

Berger, M., and H. Kaufmann, (1995): MOMS-02 -D2/STS-55 Mission. Validation of Spectral and Panchromatic Modules. Geo-Informationssysteme, 8/2, pp 21-30.

Berger, M., H. Kaufmann, and D. Meißner, (1994): Verification of spectral and panchromatic band-design of the MOMS-02 Sensor flown aboard D2/STS-55. Proc. ISPRS Symp.:, Spatial Information from Digital Photogrammetry and Computer Vision, COM-III, 2357, SPIE, Munich, FRG, pp. 43-46.

Bo-Cai, G., (1993): An operational method for estimating SNRs from data acquired with imaging spectrometers. Remote Sensing of Environment, 43, pp 23-33.

Bodechtel, J., H. Kaufmann, B. Koch, M. Berger, Q. Lei, and G. Lörcher, (1994): MOMS-02/D2 First results and future applications. International Journal of Remote Sensing, 15/13, pp. 2513-2520.

Bodechtel, J., J. Zilger, and V.V. Salomonson, (1985): Preliminary results of a quantitative comparison of the spectral signatures of Landsat TM & MOMS. Proc. of the 3rd. Int. Colloqium on Spectral Signatures in Remote Sensing, ESA SP-247, Les Arcs, France, pp. 335-341.

Hallada, A. W., J.E. Nickeson, J.A. Newcomer, and D. Strebel (1986): A comparison of MOMS and TM imaging systems, Goddard Space Flight Center, Science Applications Research, Contr. NAS 5-28200, Task Assignment 143.

Kaufmann, H., (1988): Mineral exploration along the Aqaba-Levant structure by use of TM data - concepts, processing and results. International Journal of Remote Sensing, 9/10-11, pp. 1639-1658.

Kaufmann, H., D. Meißner, J. Bodechtel, and F.-J. Behr, (1989): Design of spectral and panchromatic bands for the German MOMS-02 sensor. Photogrammetric Engineering and Remote Sensing, 55/6, pp. 875-881.

Koch, B., Th. Schneider, and U. Ammer (1993): Expected radiometric and spectral significance of MOMS-02 data for vegetation mapping - Calculations based on system parameters applied on spectral field measurements. Remote Sensing of Environment, 46, pp. 73-88.

Kneizys, F.X., E.P. Shettle, L.W. Abreu, J.H. Chetwynd, G.P. Anderson, W.O. Gallery, J.E.A. Selby, S.A. Clough, (1988): Computer code LOWTRAN-7. Air Force Geophysics Laboratory, AFGL-TR-88-0177, Hanscom AFB, MA.

Meißner, D., G. Süssenguth, et al., (1993): MOMS-02 auf D2 - Endbericht. DASA-MBB, Doc.No.: MOMS-02.RP.0100.0, München, FRG, 91 pp.

Richter, R., and F. Lehmann (1989): MOMS-02 sensor simulation and spectral band selection. International Journal of Remote Sensing, 10/8, pp. 1429-1435.

Richter, R., (1994): A spatially-adaptive fast atmospheric correction algorithm. DLR-IR 552-04/94, (also Int. Journal of Rem. Sens. in print).